Optimal management of saltwater intrusion in the coastal aquifer of Malia, Crete (Greece), using particle swarm optimization

George P. Karatzas · Zoi Dokou

Abstract Saltwater intrusion is a common phenomenon in coastal aquifers that can affect the quality of water intended for drinking and irrigation purposes. In order to provide sustainable management options for the coastal aquifer of Malia, located on the Greek island of Crete, a weighted multi-objective optimization methodology is employed. The methodology involves use of the particle swarm optimization algorithm combined with groundwater modelling. The sharp-interface approximation combined with the Ghyben-Herztberg equation is used to estimate the saltwater-intrusion front location. The prediction modelling results show that under the current pumping strategies (over-exploitation), the saltwater-intrusion front will continue to move inland, posing a serious threat to the groundwater quality. The management goal is to maximize groundwater withdrawal rates in the existing pumping wells while inhibiting the saltwater-intrusion front at locations closer to the coastal zone. This is achieved by requiring a minimum hydraulic-head value at pre-selected observation locations. In order to control the saltwater intrusion, a large number of pumping wells must be deactivated and alternative sources of water need to be considered.

Keywords Groundwater management · Coastal aquifers · Saltwater intrusion · Optimization · Greece

Introduction

Saltwater intrusion occurs in many coastal aquifers and can jeopardize groundwater quality if not detected early.

G. P. Karatzas (✉) · Z. Dokou
School of Environmental Engineering,
Technical University of Crete, Chania, 73100, Greece
e-mail: karatzas@mred.tuc.gr

Z. Dokou
e-mail: zoi.dokou@enveng.tuc.gr

Adverse results of saltwater intrusion in productive aquifers involve reduction in the available freshwater storage volume and the simultaneous contamination of production wells, given that less than 1 % of seawater (250 mg/L chloride concentration) renders freshwater unsuitable for drinking and has toxic effects on plants (Werner et al. 2013). The extent and shape of the saltwater zone depends on various parameters such as the size, shape and geological structure of the coastal aquifer as well as upstream groundwater inflow and tidal oscillations. In addition, the saltwater intrusion phenomenon is greatly enhanced by excessive groundwater pumping activity; therefore, the development of a sustainable pumping strategy is necessary to avoid the detrimental effects of unrestrained groundwater withdrawal. The first step for the determination of such a strategy depends on an accurate representation of the current saltwater intrusion extent. In many practical applications, the available data needed in order to map the saltwater wedge accurately are very limited, a fact that leads in heavy reliance on mathematical models to make estimates (Werner et al. 2013).

The evolution of the saltwater front in a coastal aquifer can be described mathematically by two main approaches: the sharp-interface and the density-dependent approach. The most simplified, widely used approach is the sharp-interface approach that can be combined with the Ghyben-Herzberg relationship under steady-state conditions. According to this approach, the physical system consists of two immiscible fluids of different constant densities (freshwater and saltwater) that form a mixing zone that is limited into an interface with a small finite width (Reilly and Goodman 1985). This approach has been applied and extended by many researchers—such as Dagan and Zeitoun (1998), Brunke and Schelkes (2001), Mantoglou (2003), Mantoglou et al. (2004), Guvanasen et al. (2000), Ababou and Al-Bitar (2004), Karterakis et al. (2007), Koukadaki et al. (2007) and Papadopoulou et al. (2010a), (2010b) among others. Under transient conditions, the behavior of the interface is controlled by both the freshwater and saltwater dynamics, since significant amounts of saltwater must enter or exit the aquifer following the interface movement (Mantoglou et al. 2004).

The density-dependent flow approach is based on the assumption that the freshwater–saltwater system consists

of a miscible fluid transporting a solute (salt) that affects the fluid properties (density and viscosity) creating a mixing zone of significant width (Pinder and Cooper 1970). Researchers have successfully applied this method in the field (Milnes and Renard 2004; Giambastiani et al. 2007; Kopsiaftis et al. 2009; Kourakos and Mantoglou 2009; Dokou and Karatzas 2012). The application of density-dependent models in real world applications, though, is a complex procedure that requires large computational effort especially when simulating complex geomorphologies. Moreover, the density-dependent method requires the knowledge of mass transport parameters such as dispersivity, that are difficult to estimate accurately and are usually determined by empiric equations or using values from the bibliography (Reilly and Goodman 1987). Consequently, the appropriateness of each method depends on the complexity of the problem at sight.

The second step towards the development of an optimal management strategy is the selection of the appropriate optimization model that, combined with the simulation model, can solve a variety of management problems taking into account economic, environmental, and societal aspects. Researchers have employed three main types of management models in order to solve the optimization problem at hand: (1) linearization methods (2) non-linear programming and (3) heuristic algorithms.

Unconfined coastal aquifers exhibit a non-linear behaviour with respect to the response of the hydraulic head to the pumping conditions, rendering the optimization problem a non-linear one. To circumvent this non-linearity researchers have used various modified versions of linear programming (Shamir et al. 1984; Uddameri and Kuchanur 2007, Karterakis et al. 2007 among others). Other researchers have employed non-linear optimization methods such as: MINOS nonlinear optimization algorithm (Gorelick et al. 1984; Willis and Finney 1988; Finney and Samsuhadi Wills 1992; Reinelt 2005 among others), sequential quadratic programming (Mantoglou et al. 2004) and the streamline upwind Petrov-Galerkin formulation (Gordon et al. 2000).

However, conventional optimization algorithms using non-linear programming sometimes have difficulty in finding the global optima or, in case of multi-objective optimization, the Pareto front. Thus, in recent years, research has been directed towards heuristic techniques, such as evolutionary algorithms, Tabu search and simulated annealing due to their broad applicability to general management scenarios. Various applications in saltwater intrusion management have applied such algorithms successfully (Cheng et al. 2000; Cai et al. 2001; Karterakis et al. 2007; Mantoglou and Papantoniou 2008; Dhar and Datta 2009; Kourakos and Mantoglou 2011).

Saltwater intrusion is as a problem with multiple conflicting objectives, i.e. maximization of groundwater extraction while satisfying environmental criteria. This multi-objective problem is solved here using the particle swarm optimization (PSO) algorithm in a weighted average approach. The effectiveness of the PSO algorithm

has not yet been tested in saltwater intrusion applications, which constitutes the novel contribution of this work. Specifically, the approach employed here is to combine a groundwater flow simulation model that defines the location of the saltwater intrusion toe based on a hydraulic approach (sharp interface and Ghyben-Herztberg approximation) with PSO. The optimization goal is to maximize groundwater withdrawal in the existing pumping well network while inhibiting saltwater intrusion in the coastal aquifer. All pumping scenarios attempt to find a balance between socioeconomic (i.e. the water needs of the local communities) and environmental (saltwater mitigation) factors. The study area where the aforementioned methodology is applied and tested is the coastal aquifer of Malia located on the island of Crete, Greece, where the phenomenon of groundwater overexploitation is intense, especially during the summer months.

Methodology

Groundwater simulation model: PTC

Princeton transport code (PTC) is a three-dimensional (3D) groundwater flow and contaminant transport simulator that uses a combination of finite element and finite difference methods to solve a system of partial differential equations that represent the groundwater flow, velocity and contaminant mass transport of the simulated physical system (Babu et al. 1997):

$$\nabla \cdot (\mathbf{K} \cdot \nabla h) = 0 \tag{1}$$

$$\frac{\partial c}{\partial t} - \nabla \cdot (\mathbf{D} \cdot \nabla c) - \nabla \cdot (\mathbf{v} c) = 0 \tag{2}$$

$$\mathbf{v} = -\frac{\mathbf{K}}{n} \nabla h \tag{3}$$

In Eqs. (1), (2) and (3), h is the hydraulic head, $\mathbf{K}$ is the tensor of hydraulic conductivity, $\mathbf{D}$ is the tensor of hydrodynamic dispersion, c is the solute concentration, t is time, $\mathbf{v}$ is the pore velocity vector, and n is the effective porosity.

The preceding system of equations includes the following: the steady state flow of water through a porous medium (Eq. 1), the transport equation that describes the contaminant concentration migration with time (Eq. 2) and a constitutive relationship between groundwater pore velocity and hydraulic head (Darcy's law, Eq. 3).

PTC employs a splitting algorithm for solving the fully 3D equations which provides considerable savings both in

computer memory requirements and computational effort. The domain is discretized into approximately parallel horizontal layers. Within each layer a finite element discretization is used allowing for accurate representation of irregular domains. The vertical connection of the layers is accomplished using finite difference discretization. This hybrid coupling of the finite element and finite difference methods provides the opportunity to divide the computations into two steps during a given time iteration (splitting algorithm). In the first step, all the horizontal equations are solved using finite elements, while in the second step, the vertical equations which connect the layers are solved using finite differences (Babu et al. 1997). PTC is coupled with a graphical user interface (GUI) called ArgusOne that is an easy-to-use GIS-based graphical pre- and post-processor. This model has been successfully used in several previous studies (Aivalioti and Karatzas 2006; Koukadaki et al. 2007; Dokou and Pinder 2011).

In this work, the PTC model was used in conjunction with the sharp interface approach and the Ghyben-Herztberg approximation in order to estimate the saltwater intrusion extent, as discussed in detail in the following. According to this approach only the hydraulic head values on the model domain are needed in order to approximate the saltwater intrusion extent; thus, only the flow module of the PTC algorithm was employed here.

Sharp-interface approach

This approach is based on the assumption that the mixing zone between two immiscible fluids with different constant densities (fresh and saline water) is limited into an interface of a small finite width. The location of the sharp interface between the two fluids is determined by the difference between the hydraulic heads of the saline water and freshwater and the volume of freshwater flowing towards the shoreline from inland (Reilly and Goodman 1985). Based on the sharp interface theory, the physical system is modelled using only the standard groundwater flow equation and the seawater intrusion front is approximated hydraulically using the Ghyben-Herzberg relationship developed independently by Ghyben (1888) and Herzberg (1901) around the same time:

$$\xi = \frac{\rho_f}{\rho_s - \rho_f} h_f \approx 40 h_f \qquad (4)$$

In Eq. (4), ξ is the interface depth below the sea level, h_f is the hydraulic head of the freshwater above the sea level, ρ_f is the density of freshwater (1,000 kg/m^3), and ρ_s is the density of saline water (1,025 kg/m^3).

This means that for the aforementioned freshwater and saltwater densities, for each meter of freshwater hydraulic head (h_f) above the mean sea level, the interface between saline water and freshwater is balanced approximately 40 m below the mean sea level.

It has been shown by previous studies (Llopis-Albert and Pulido-Velazquez 2014) that the sharp interface approximation is reasonable regarding regional-scale problems when the transition zone is narrow relative to the scale of the problem. Additionally, they have shown that higher values of layer thickness, longitudinal dispersion coefficients, and molecular diffusion coefficients, as well as lower values of recharge, transmissivity, and distance of the wells to coast, lead to a better approximation using the sharp interface approach (Llopis-Albert and Pulido-Velazquez 2014). Finally, this approach is more suitable for modeling long-term responses of freshwater lenses or short-term responses in aquifers where seawater can move in and out easily (Mantoglou et al. 2004). The interested reader is directed to Reilly and Goodman (1985), Bear (1999) and Diersch and Kolditz (2002) for an extensive review on the sharp interface approach.

Optimization problem formulation

The objective of the optimization algorithm is to maximize the total water withdrawal while controlling the location of the saltwater intrusion front. Constraints that ensure no further intrusion of the seawater front are imposed at pre-selected observation locations where the calculated hydraulic head should be greater than a minimum value (h_{min}). This value is calculated by the Ghyben-Herzberg relationship. Restrictions for all the production wells regarding the maximum allowable extraction rate were also set equal to the current extraction rates (Q_{imax}). The mathematical formulation of the problem is described by the following equations:

$$\max \sum_{i=1}^{n} Q_i \qquad , \ i = 1, \ldots, n \qquad (5)$$

subject to:

$$h_j \geq h_{min} \qquad , \ j = 1, \ldots, m \qquad (6)$$

$$Q_i \leq Q_{imax} \qquad (7)$$

$$Q_i \geq 0 \qquad (8)$$

In Eqs. (5)–(8), n is the number of production wells, m is the number of observation locations where a head constraint is imposed, Q_i is the pumping rate of well i, Q_{imax} is the maximum allowable extraction rate for each well i, h_j is the hydraulic head at a control location j, h_{min}

is the minimum hydraulic head needed to avoid saltwater intrusion in the aquifer.

Due to the fact that PSO cannot solve constrained problems, the constrained optimization problem described in the preceding was reformulated into an unconstrained problem as follows:

$$\min f(Q) = \begin{cases} -w_1 \sum_{i=1}^{n} Q_i + w_2 \sum_{j=1}^{m} (h_{min}-h_j), & \text{if } h_{min}-h_j \leq \varepsilon \\ -w_1 \sum_{i=1}^{n} Q_i + w_2 \sum_{j=1}^{m} (h_{min}-h_j) + w_3, & \text{if } h_{min}-h_j > \varepsilon \end{cases},$$

$$i = 1,\ldots n \text{ and } j = 1,\ldots m \qquad (9)$$

In Eq. (9), w_1 and w_2 are weights that are used as scaling factors in order to assign relatively equal importance between the two criteria of the objective function. The negative sign of the first term in each equation indicates maximization. The parameter w_3 is a penalty imposed whenever the constraint of maintaining a minimum hydraulic head is not satisfied in any of the preselected control locations. Note that the difference of $h_{min}-h_j$ is given a tolerance ε (in this work $\varepsilon=0.01$ m, since a difference of 1 cm in hydraulic head can be considered negligible) before the penalty is imposed. The upper and lower bound constraints remain active for this alternative formulation.

PSO algorithm

In the unconfined aquifer studied in this work, the optimization of pumping activity is nonlinear due to the nonlinear relation of the groundwater system to the pumping stress under water-table conditions. Specifically, according to the Dupuit-Forchheimer equation for unconfined aquifers, the hydraulic head calculation at any location of the unconfined aquifer is a nonlinear function of the hydraulic head at a known distance from the pumping well. This makes evolutionary algorithms such as PSO, an attractive method for solving this non-linear optimization problem.

The PSO algorithm, developed by Eberhart and Kennedy (1995), was inspired by the behavior of swarms of animals. According to this method, each individual behaves as a particle in multidimensional space with a specific position and velocity. During each iteration, a particle in a specific point in space moves to a new one by adding a velocity to its current position, keeping track of the best position it has achieved so far. All particles are members of what is called a swarm. The particle velocity is determined by three components: the *inertia component*, causing the particle to continue moving in one direction, the *cognitive component*, causing the particle to move towards the best position it has ever been in and the *social component,* steering the particle towards the best position of any particle of the swarm (global best) or in its

neighborhood (local best). The particle position and velocity are calculated according to the following equations:

$$\mathbf{v}_i(t) = \mathbf{v}_i(t-1) + \varphi_1 \text{rand}_1 \cdot (\mathbf{p}_i - \mathbf{x}_i(t-1)) \qquad (10)$$
$$+ \varphi_2 \text{rand}_2 \cdot \left(\mathbf{p}_g - \mathbf{x}_i(t-1) \right)$$

$$\mathbf{x}_i = \mathbf{x}_i(t-1) + \mathbf{v}_i(t) \qquad (11)$$

In Eqs. (10) and (11), $\mathbf{v}_i$ is the velocity of particle i, $\mathbf{x}_i$ is the position of particle i, $\mathbf{p}_i$ is the best position of particle i, $\mathbf{p}_g$ is the global best position of all particles, t is the current iteration number, ϕ_1 and ϕ_2 are two positive numbers (acceleration constants), and rand$_1$ and rand$_2$ are two uniformly distributed random numbers in the range of [0,1].

During the implementation of the particle swarm optimization there are certain parameters that need to be taken into account in order to avoid the "explosion" of the swarm, to speed convergence and to avoid premature convergence (swarm collapse). These include the selection of the maximum velocity, the acceleration constants, the constriction factor (del Valle et al. 2008) and the selection of neighborhood topology (if a local search is implemented). Various methods have been proposed in order to define these parameters and solve the associated problems. A selection of those is chosen and applied here.

More specifically, the maximum velocity was chosen to be limited using a multiplier that is usually between 0 and 1, as follows:

$$v_{max} = k x_{max} \qquad (12)$$

where k is the velocity multiplier and x_{max} the variable's upper bound.

It has been found empirically that, even when the maximum velocity and the acceleration constant are defined correctly, the particles may still diverge. The method selected in this work to overcome this problem is the constriction factor method first proposed by Clerc and Kennedy (2002). This method updates Eq. (10) as follows:

$$\mathbf{v}_i(t) = \chi \cdot \begin{Bmatrix} \mathbf{v}_i(t-1) + \varphi_1 \text{rand}_1 \cdot (\mathbf{p}_i - \mathbf{x}_i(t-1)) \\ + \varphi_2 \text{rand}_2 \cdot \left(\mathbf{p}_g - \mathbf{x}_i(t-1) \right) \end{Bmatrix} \qquad (13)$$

$$\chi = \frac{2}{\left| 2 - \varphi - \sqrt{\varphi^2 - 4\varphi} \right|}, \quad \varphi = \varphi_1 + \varphi_2 > 4 \qquad (14)$$
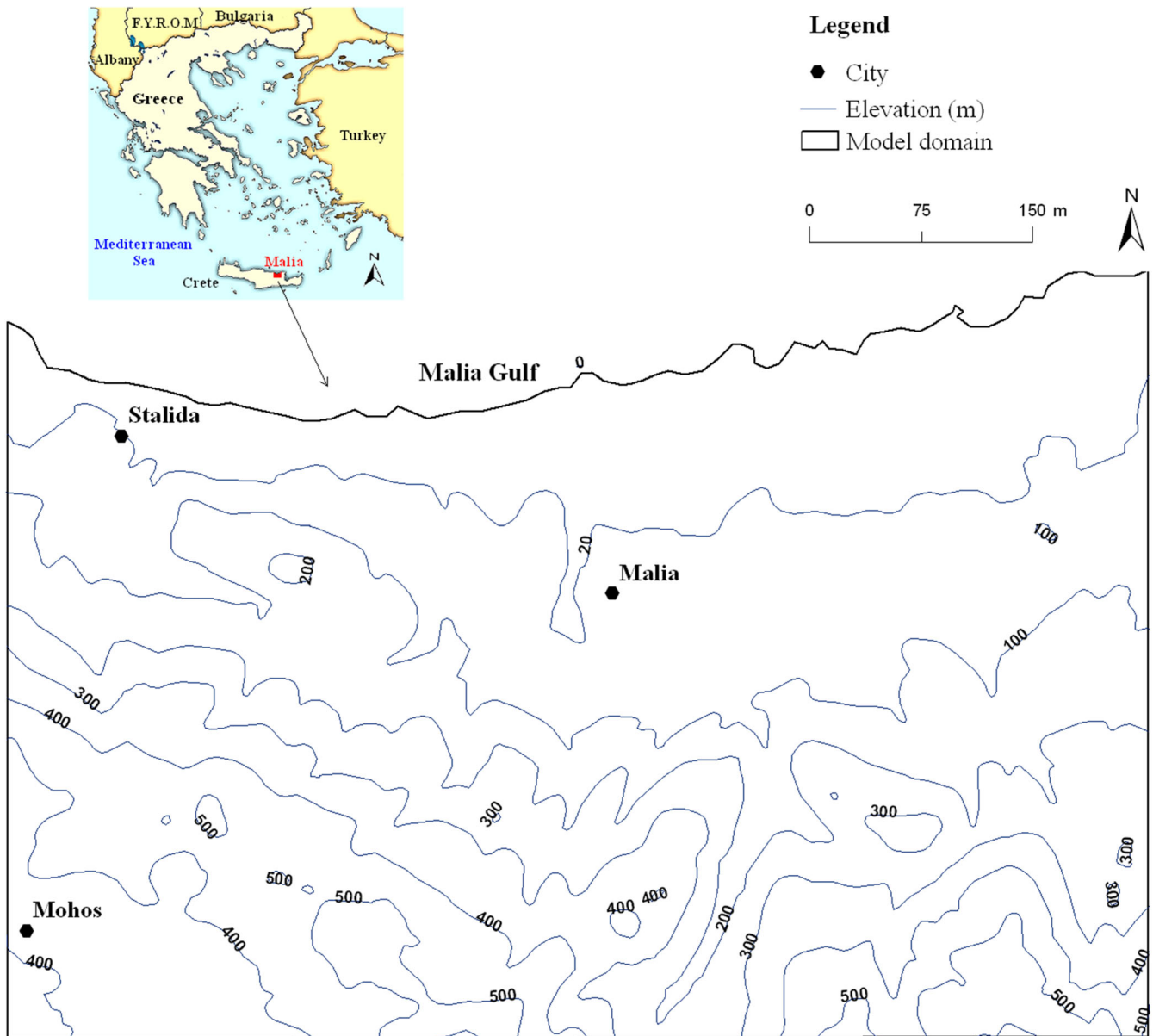
Fig. 1 Map of study area location and topography

It has been shown empirically that the optimal values for this method are $\phi_1 = \phi_2 = 2.05$; thus, the constriction factor equals $\chi = 0.729$ (del Valle et al. 2008).

In this application, global best PSO was first applied but at around the 50th iteration premature convergence was detected, with all particles collapsing to a single point. Thus, local best PSO was adapted using ring topology, meaning that each particle can communicate information between only two other particles (neighbors). The primary purpose of using neighbors instead of exchanging information between the entire swarm is to preserve diversity and allow the particles to explore larger areas without immediately being drawn to the global best solution.

The coupling between the groundwater flow simulator and the optimization model is achieved as follows—for each member of the swarm containing a potential solution of pumping rates for each well, a call is made to the simulator that calculates the hydraulic head at the preselected observation locations where a minimum head is required. Then, the corresponding objective function value (fitness) is calculated and stored.

The main advantage of PSO over other evolutionary computation algorithms such as the genetic algorithm (GA), lies in the fact that in PSO there exist two populations (the local bests and the current positions). This allows greater diversity and exploration over a single population. In addition, PSO converges faster than GA due to the momentum effects on particle movement (e.g. when a particle is moving in the direction of a gradient).

Elbeltagia et al. (2005) compares five evolutionary-based algorithms: GA, memetic algorithms, PSO, ant-
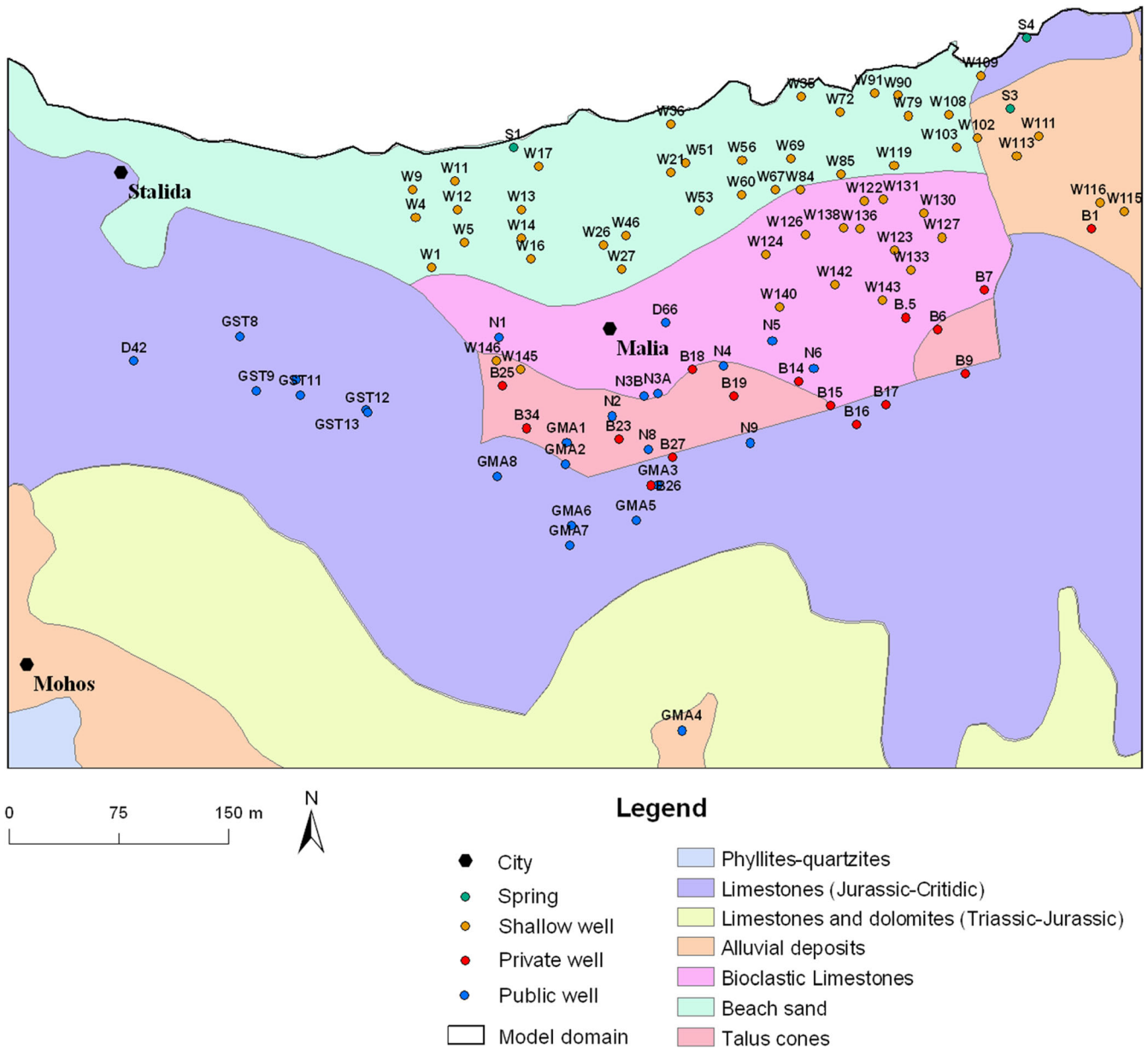
Fig. 2 Geological formations and wells located in the study area

colony systems, and shuffled frog leaping. They concluded that the PSO method was generally found to perform better than other algorithms in terms of success rate and solution quality, while being second best to ant-colony systems in terms of processing time. Dokou and Karatzas (2013) also found PSO to be superior to genetic algorithm (GA) and differential evolution (DE) algorithms in a groundwater application.

Although other similar optimization algorithms such as genetic algorithms, differential evolution etc., have been used frequently in real world subsurface hydrology problems, the PSO method has been recently applied in only a few works (Matott et al. 2006; Tian et al. 2011; Gaur et al. 2011; Dokou and Karatzas 2013) and has never been applied in saltwater intrusion management studies previously.

Field application

The optimization algorithm was applied in order to manage saltwater intrusion in the aquifer of Malia, located in northern Crete, 40 km east of the city of Heraklion. The study area is characterized by a gentle slope to the north of the town of Malia and by mountains to the south. The elevation varies from 0 to 200 m above mean sea level (amsl) over the coastal lowland and from 200 to 550 m amsl over the area south of the city of Malia and towards the south (model domain). The location of the study area in Greece and the boundaries of the model domain are shown in the topographical map of the area presented in Fig. 1. The mountainous terrain continues to the south of the model boundary reaching a maximum elevation of 1,400 m over the Selena area. The
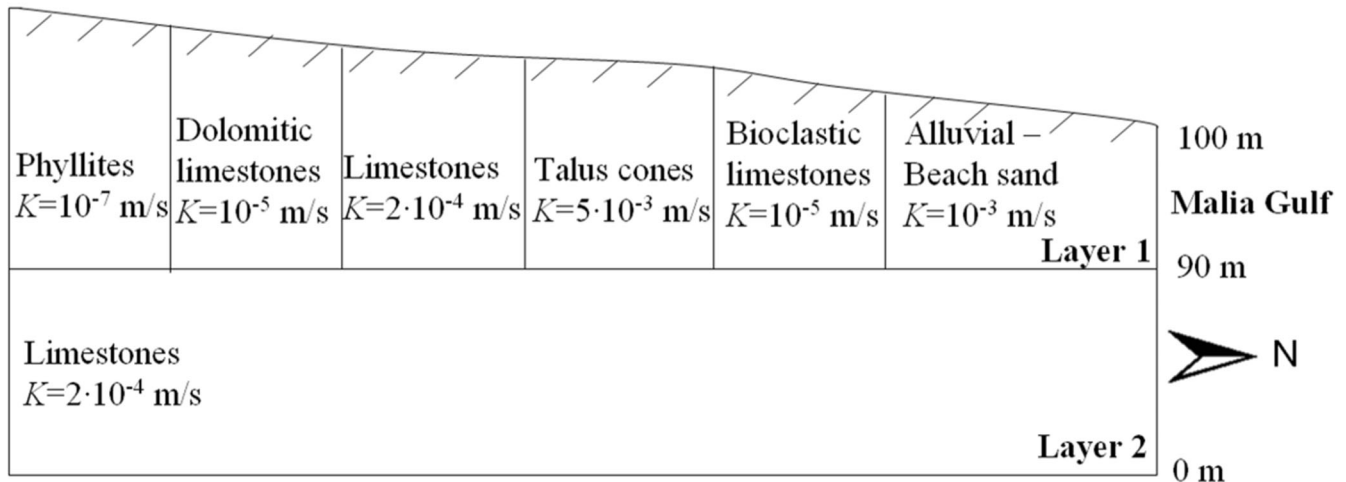
650 m

Fig. 3 Vertical discretization of the model and calibrated hydraulic conductivity (K) values for each geological formation

cultivated area of the municipality of Malia is 1.75 km². Sclerophyllous vegetation and complex cultivation patterns cover most of the study area. Other land uses include olive groves, natural grassland, non-irrigated arable land and a small area of discontinued urban fabric around the towns of Malia and Mohos.

The coastal karstic aquifer of Malia is developed in limestones of the Tripolis zone. Under these rocks, a series of alternating chloritic schists, phyllites and quartzites belonging to the Phyllite-Quartzite zone acts as the impermeable substrate of the extended region (Kallergis et al. 2000). The Tripolis series consists of faulted and karstified limestones, dolomites and calcareous dolomites (Jurassic-Critidic and Triassic-Jurassic) as shown in the geological map of Fig. 2. The stratigraphy includes Neogene deposits that consist of bioclastic Messinian limestones and Quaternary clastic sediments. Along the coast, alluvial deposits and beach sand deposits are found (Quaternary deposits).

Groundwater flow model development

Model discretization
The horizontal discretization of the study area was implemented using a triangular finite element mesh consisting of 3,017 nodes and 5,831 elements. The

vertical discretization of the model area (Fig. 3) was based on information obtained from boring logs in conjunction with the geological map of the area. Boring logs were available only for public wells GMA1, GMA3, GMA4, GMA5, GMA6, GMA7, GMA8, GST8, GST9, GST11 and GST12, but are not shown here for brevity. The conceptual model comprised an unconfined aquifer of 100 m depth, which was discretized into 2 layers. The top layer of the model follows the topography of the area (variable elevation of 0–550 m), while the elevation of the bottom layer was set at −10 m (amsl). PTC does not handle negative elevations very well, thus, the aquifer's depth of 100 m was added to all the elevations, hydraulic head values etc. After this transformation, the elevation at sea level is 100 m, the top layer elevation varies from 100 to 650 m, the top elevation of the bottom layer of the model is 90 m and the bottom of the aquifer is at 0 m (Fig. 3).

Hydraulic conductivity
The transmissivity (T) for various locations was determined from pumping tests conducted in the aquifer of interest by Kallergis et al. (2000). Information regarding the aquifer-test parameters and results is provided in Table 1. The values represent the average results of the Theis and Jacob methods of analysis. Transmissivity varies from 0.78 to 61.02 m²/h for limestone formations (Kallergis et al. 2000). The preceding results were taken into account when the hydraulic conductivity (K) parameter was fine-tuned during the process of model calibration. The final calibrated K values that were used in the model are presented in Fig. 3.

Aquifer recharge due to rainfall
The spatial distribution of rainfall data in the area was estimated using measurements from three meteorological

Table 1 Aquifer test results (Kallergis et al. 2000). *NA* not available

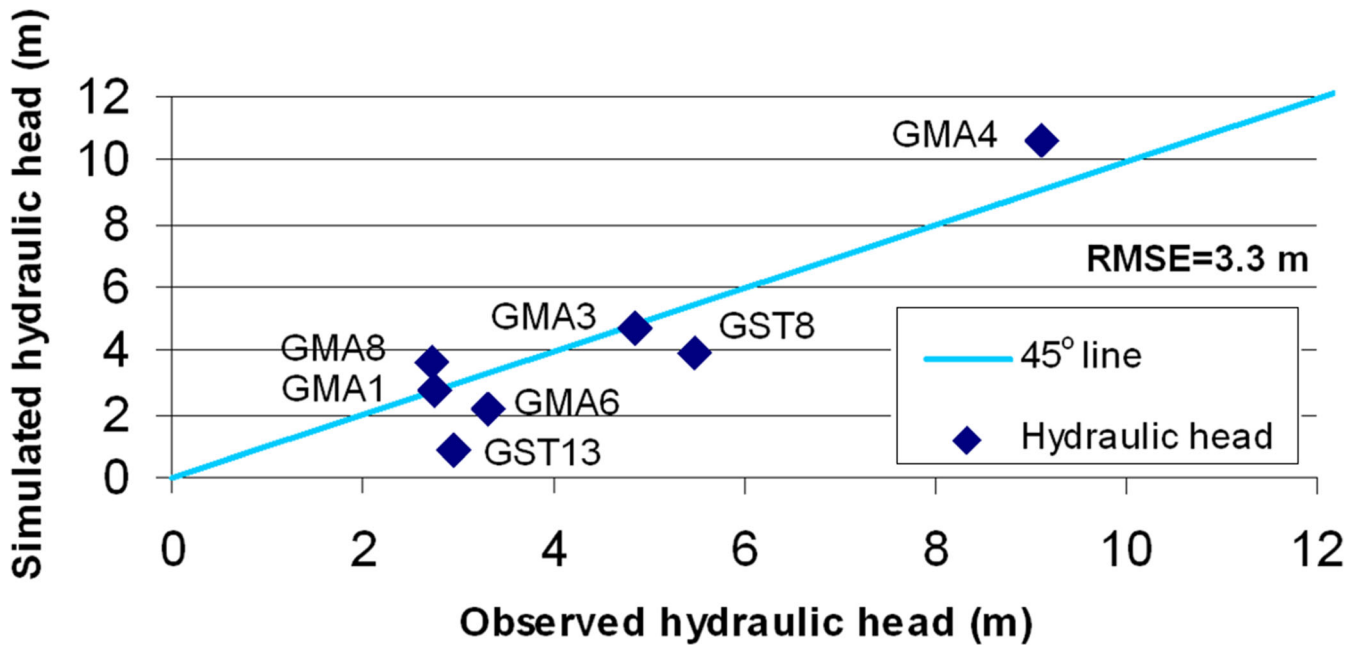| Well name	Tapping depth (m)	Duration (h)	Q (m³/h)	Transmissivity (m²/h)
GMA1	92	10	60	61.02
GMA3	125	24	60	43.65
GMA4	255	NA	50	0.78
GMA7	230	12	90	19.32
GMA9	178	30	24	9.75
GMA11	197	30	20	1.09

Fig. 4 Comparison between observed and simulated hydraulic heads in seven wells

stations (Neapolis, Avdou, Kasteli) located inside or very close to the study area for the period of October 1995 to November 2011, which corresponds to the model simulation period. Each year was divided into a wet (October–March) and a dry (April–September) period, each consisting of 6 months. An average value for each wet and dry period of each year was then used as a rainfall value. Using the average rainfall values measured at these stations provides a better representation of the conditions in the area rather than using the data from only one meteorological station. The amount of rainfall that penetrates the ground surface (infiltration) and eventually reaches the groundwater (recharge) depends on the soil moisture, lithology, slope, vegetation etc. For the estimation of the percentage of rainfall that represents recharge for each geological formation, typical values were used that were provided by Kallergis et al. (2000) in their hydrological report of the Malia region and are representative of the study area. These values are 44 % for the limestone formations, 21.5 % for the neogenic sediments, 15 % for Quaternary deposits and 5 % for phyllites.

Boundary and initial conditions
The exploitation of the aquifer system is realized by a great number of wells. Information for 49 shallow wells with depths from 2 to 20 m (starting with the letter W), 8 private (starting with the letter B) and 24 public wells (starting with GMA, GST, N and D) was available for this study (a total of 81 pumping wells). Their locations were presented in Fig. 2.

The groundwater drainage is observed to occur in a northerly direction, while the aquifer is recharged mainly from the mountainous regions through the carbonate

rocks. A first type flow boundary condition was set along the coastline, setting the hydraulic head to 100 m along the coastline. Pumping wells in the area of interest were defined as second type boundary conditions assuming that their screens are located at the top layer (layer 2). Specific information regarding the well screens was not available. Pumping is assumed to occur only during the dry summer period, when the irrigation and drinking water needs are at maximum. Three brackish springs are located in the area (S1, S3 and S4). The discharge from the three springs was also included in the model as a second type boundary condition. In addition, time-dependent flowrates (in m^3/day) that vary seasonally were defined on parts of the southern and eastern model boundaries as a result of the calibration process. These boundary conditions represent the inflow to the model domain that occurs from adjacent groundwater basins. Initial conditions were set for the beginning of the simulation (October 1995) by interpolating field measurements that were collected at that time.

Model calibration
The calibration of the flow field was based on hydraulic head data measured in 7 wells in November 2011. The parameters that were varied during the calibration procedure included the hydraulic conductivity values for the various geologic formations and the lateral influx rates on the southern and eastern model boundaries. The flow calibration results show a good agreement between measured and model values in most cases (Fig. 4). The R^2 value for the comparison between data and model results is 0.93, and the corresponding root mean square error (RMSE) is equal to 3.3 m, indicating an acceptable fit.
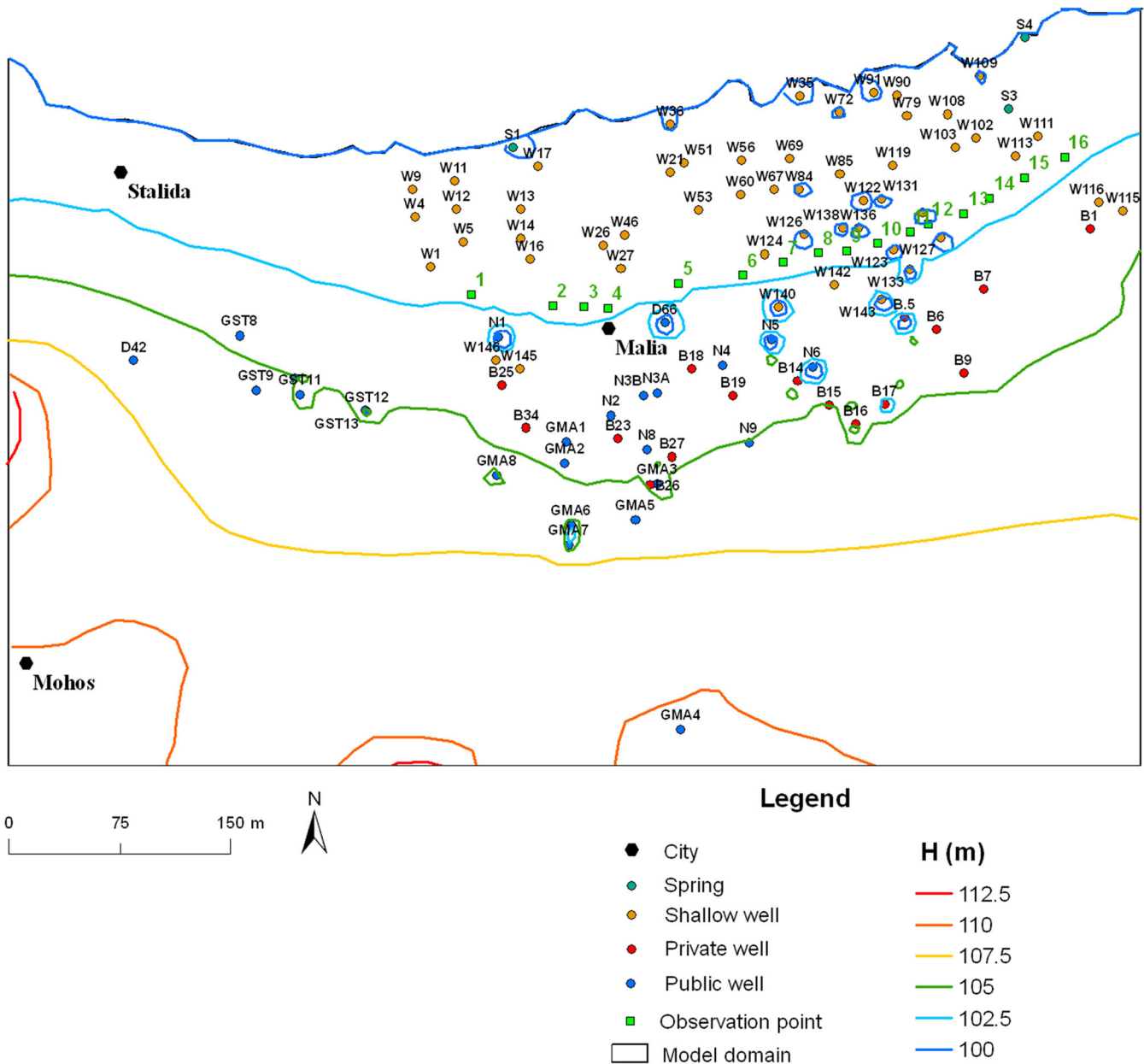
Fig. 5 Hydraulic head (*H*) calibration results, location of saltwater-intrusion front (102.5 m) under future conditions, and control points (*1–16, green squares*)

Saltwater intrusion estimation

The model was also used to predict future aquifer conditions, projecting the aquifer state 10 years in the future and the location of the saltwater intrusion front according to the sharp interface approach, if groundwater extraction continues with the current scheduling (assuming no water resources management strategy for the inhibition of the saltwater intrusion front) is shown in Fig. 5, representing the worst-case scenario. In this case study, the depth of the modeled aquifer is approximately 100 m below sea level (ξ=100 m); thus, according to the Ghyben-Herzberg relationship, the hydraulic head of the freshwater at the interface should be h_f=2.5 m. This means that as long as the equivalent hydraulic head of

freshwater remains 2.5 m above sea level (or 102.5 m for the model), the movement of saltwater into the coastal aquifer can be avoided.

Optimization problem formulation

The prediction model, which was based in the calibrated PTC model for the area, was used in conjunction with the optimization algorithm in order to select an optimal management strategy for the saltwater intrusion problem in the area, under two scenarios, described in detail in the following. The weights used for each conflicting objective were set to w_1=0.00001, w_2=1, w_3=5 (penalty), in order to balance the two objectives and ensure they are in the same

Table 2 Optimal extraction rates and objective function value for scenario 1

Well name	Upper bound (m³/day)	Optimal rate (m³/day)
B9	1,680	0
B1	1,200	0
B16	1,200	0
B17	1,440	0
B18	960	0
B5	960	0
B6	960	0
B7	960	0
D42	240	0
D66	1,200	0
GMA1	1,560	0
GMA2	2,400	0
GMA3	1,440	1,440
GMA4	480	480
GMA5	960	0
GMA6	1,296	0
GMA7	960	960
GMA8	720	0
GST8	264	0
GST9	288	288
GST11	552	0
GST12	768	768
GST13	312	0
N1	1,200	0
N2	1,440	0
N3A	1,440	0
N3B	1,440	0
N4	1,440	0
N5	1,200	1,200
N6	1,440	0
N8	2,040	0
N9	240	0
W1	960	0
W102	360	0
W103	360	0
W109	360	0
W11	360	0
W111	2,400	0
W113	480	0
W115	480	253.38
W116	600	0
W119	720	0
W12	480	0
W122	600	0
W123	600	0
W126	480	0
W127	480	0
W13	360	0
W130	480	0
W131	480	0
W133	480	0
W136	480	0
W138	480	0
W14	960	0
W140	720	720
W143	720	720
W145	960	0
W146	960	0
W16	480	0
W17	1,064	1,064
W206	480	480
W21	360	360
W26	480	0
W27	360	0
W35	360	360
W36	480	480
W4	600	0
W46	480	0
W5	600	0
W51	480	480
W53	480	0
W56	480	480
W60	720	0
W67	720	720
W69	360	0
W72	480	0
W79	480	0
W84	720	720
W85	720	0
W9	480	0
W91	480	0

Total extraction rate (m³/day): maximum 63,824, optimal 11,973.38; optimal objective function value: −0.1001

order of magnitude. A population of 25 particles was used in each generation, and a maximum number of 100 iterations was defined as the stopping criterion, corresponding to 2,500 calls to the simulation model. The initial population was created randomly. In order to select the parameter values that would produce the best results, the relevant literature was consulted (del Valle et al. 2008). The final values that gave the best results were the velocity multiplier k=0.3 and ϕ_1=ϕ_2=2.05 (corresponding to a constriction factor of χ=0.729). The hydraulic head is constrained at a minimum of 102.5 m at 16 control locations shown in Fig. 5, which represent an attempt to mitigate the saltwater intrusion front closer to the shore as compared to the location predicted under future conditions if the wells continue to pump with the same rates. The upper bounds of the pumping rates for each well were set to the current extraction rates presented in Table 2.

Results and discussion

Scenario 1

For scenario 1, all 81 pumping wells that are currently active in the area were included in the optimization

Table 3 Computed hydraulic heads at constraint locations using the optimal solution for scenarios 1 and 2

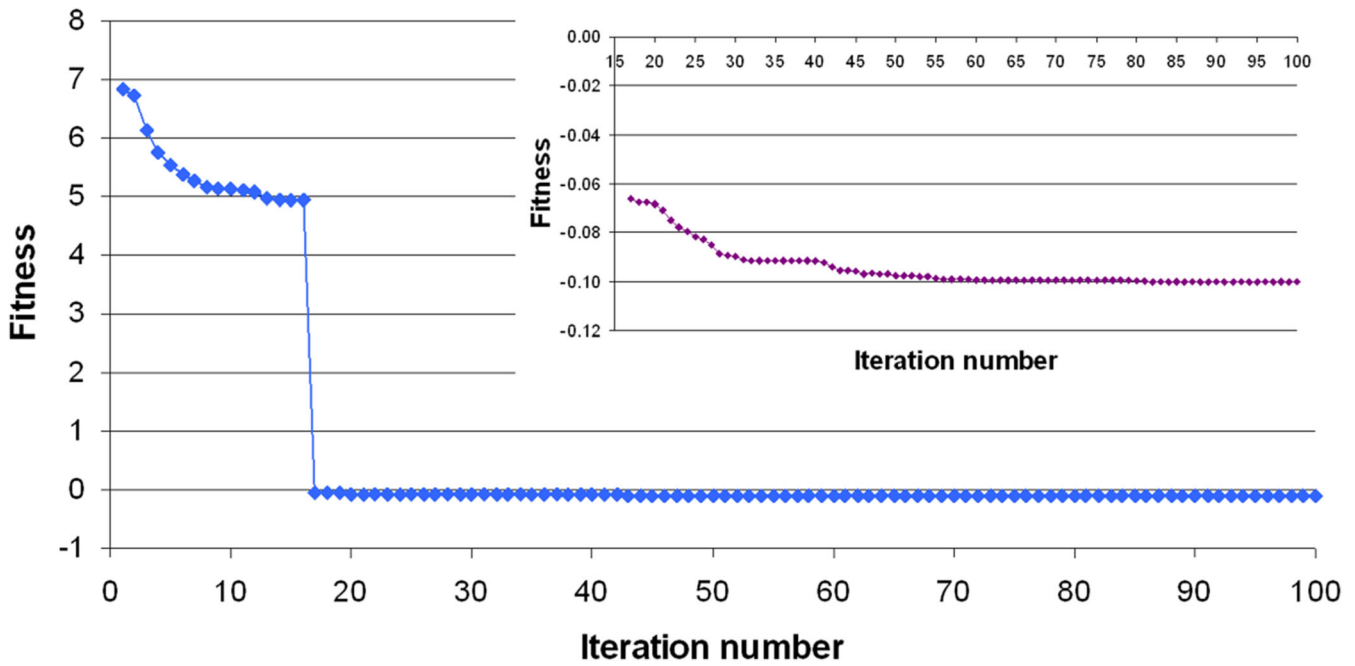| Constraint No.	Computed hydraulic head (m)	
	Scenario 1	Scenario 2
1	102.60	102.59
2	102.49	102.50
3	102.49	102.50
4	102.54	102.55
5	102.68	102.72
6	102.69	102.76
7	102.54	102.62
8	102.51	102.58
9	102.58	102.65
10	102.65	102.71
11	102.61	102.65
12	102.59	102.62
13	102.60	102.62
14	102.50	102.50
15	102.51	102.50
16	102.66	102.63

Fig. 6 Convergence rate of the algorithm under scenario 1. *Inset* shows enlarged scale from iteration number 17 onward

process. The optimal solution obtained by the algorithm is presented in Table 2. The optimal objective value achieved by the algorithm is −0.1001. It is observed that in order to achieve the necessary target hydraulic head at the observation locations, a vast number of wells are completely shut down by the algorithm (63 inactive wells and only 18 remaining active). The total extraction rate is reduced to 11,973.38 m³/day, which corresponds only to 18.75 % of the current production rate.

The hydraulic heads at the constraint locations are shown in Table 3. It is observed that the constraint of 102.5 m is satisfied in all locations, while for points 2 and 3 the tolerance of 0.01 m has become effective. This fact increases the objective value by a small amount ($w_2 \cdot 0.02$) but the penalty of 5 is deactivated.

The convergence rate of the algorithm is presented in Fig. 6. The penalty imposed for not satisfying the hydraulic head constraints is active until the 16th iteration. From the 17th iteration forward, the objective function drops to negative values, since the penalty is no longer active. The algorithm converges to the optimal value on the 83rd iteration.

Scenario 2

Given the fact that the water pumped from wells located inside the saltwater-intruded zone is of questionable quality, for scenario 2, only the wells that are located outside the saltwater-intruded area are allowed to extract groundwater; thus, only 33 out of the 81 production wells are considered for this scenario. The optimal objective value achieved by the algorithm is −0.1089, which is a little better compared to scenario 1. This is due to the fact that according to this solution, all hydraulic heads at the

Table 4 Optimal extraction rates and objective function value for scenario 2

Well name	Upper bound (m³/day)	Optimal rate (m³/day)
B1	1,200	0
B5	960	0
B6	960	0
B7	960	0
B9	1,680	0
B16	1,200	0
B17	1,440	0
D42	240	240
D66	1,200	0
GMA1	1,560	0
GMA2	2,400	0
GMA3	1,440	1,440
GMA4	480	480
GMA5	960	960
GMA6	1,296	1,296
GMA7	960	960
GMA8	720	0
GST8	264	264
GST12	768	768
GST13	312	312
N1	1,200	0
N2	1,440	0
N3A	1,440	0
N3B	1,440	0
N4	1,440	0
N5	1,200	1,200
N6	1,440	1,440
N8	2,040	0
N9	240	240
W115	480	174.21
W116	600	600
W145	960	0
W146	960	0

Total extraction rate (m³/day): 10,374.21; optimal objective function value: −0.1089
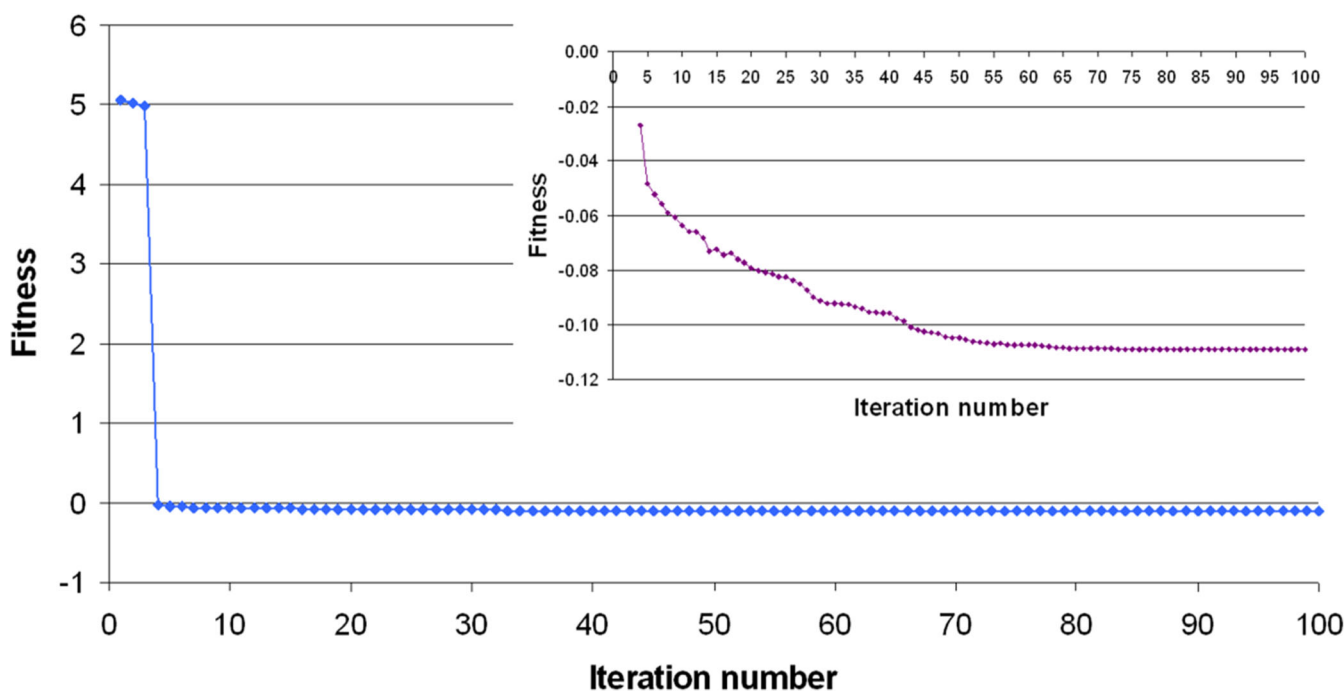
Fig. 7 Convergence rate of the algorithm under scenario 2. *Inset* shows enlarged scale from iteration number 4 onward

16 control locations achieved the specified target of 102.5 m (Table 3) without the tolerance of 0.01 m being activated.

The optimal strategy (Table 4) indicates that in order to achieve the target hydraulic head at the control locations, 14 out of 33 wells remain active and 19 wells are shut down. The total extraction rate achieved by this solution is 10,374.21 m^3/day, slightly smaller than the total extraction rate of scenario 1 (16.25 % of the current extraction rate). The main difference is that all wells pump freshwater and not brackish water of variable salinity, making this scenario a more attractive management strategy. The total extraction rate remains small, indicating that alternative sources of water for drinking and irrigation needs have to be considered in the area in order to achieve sustainable management of water resources. Comparing the two scenarios, 6 out of 14 of the wells that are kept active are the same (GMA3, GMA4, GMA7, GST12, N5, W115), indicating that these wells affect the saltwater intrusion phenomenon the least. This is mainly due to their location, which is far from the shoreline for all wells except W115, which is located close to the model boundary. Note that in both scenarios 1 and 2, well W115 is selected as pumping location with the pumping rate within the desired range, while for the rest of the wells, the optimal pumping values equal either their lower or upper bounds. This effect is probably due to a boundary effect, given the W115 well's proximity to it.

The convergence rate of the algorithm for scenario 2 is presented in Fig. 7. This time the penalty for not satisfying the hydraulic head constraints remains active only up to the 3rd iteration. From the 4th iteration forward, the objective function drops to negative values, since the penalty is no longer active. The algorithm converges to the optimal value on the 73rd iteration, although it has reached a very similar value at the 64th iteration.

Conclusions

In this work, the coastal aquifer of Malia, located in the northern part of Crete, Greece, is studied in order to identify the current and future extent of saltwater intrusion and formulate alternative management plans for mitigation of the phenomenon. The groundwater-flow modelling results show that under the current pumping strategy, the saltwater intrusion front will continue to move inland posing a serious threat for the groundwater quality used for drinking and irrigation purposes. For this reason, two optimal management scenarios for mitigation of the saltwater intrusion phenomenon were considered. The first scenario allowed all pumping wells in the area to extract water with an upper bound equal to the current extraction rates. The optimization results that were obtained using the PSO algorithm indicate that only 22.2 % of the 81 production wells remain active limiting the amount of extracted groundwater to 18.75 % of the current rate. For the second scenario only the wells that are located outside the saltwater-affected areas are considered, given the fact that the water extracted from wells located inside the affected zones provide water of questionable quality. According to this scenario, 42.4 % of the 33 wells remain active and provide a water volume that corresponds to 16.25 % of the current rate. The main difference between the two scenarios is that the second scenario guarantees that the water extracted is of higher

quality, making it a more attractive management strategy for mitigating the saltwater intrusion phenomenon, while providing better quality water to the region. It is observed that, in both cases, the total extraction rate remains extremely small; thus, alternative sources of water for satisfying the drinking and irrigation needs of the region need to be investigated in order to achieve sustainable management of the water resources. In addition, the low extraction rates needed to mitigate the phenomenon confirm the slow nature of the saltwater intrusion process, requiring a long time for the saltwater front to adapt to management scenarios. This makes the phenomenon very difficult if not impossible to reverse, indicating that management options should focus more on prevention rather than on mitigation measures.

References

Ababou R, Al-Bitar A (2004) Salt water intrusion with heterogeneity and uncertainty: mathematical modeling and analyses. Dev Water Sci 55:1559–1571

Aivalioti MV, Karatzas GP (2006) Modeling the flow and leachate transport in the vadose and saturated zone: a field application. Environ Model Assess 11(1):81–87

Babu DK, Pinder GF, Niemi A, Ahlfeld DP, Stothoff SA (1997) Chemical transport by three-dimensional groundwater flows. 84-WR-3, Princeton University, Princeton, NJ

Bear J (1999) Conceptual and mathematical modeling. Kluwer, Dordrecht, The Netherlands

Brunke H-P, Schelkes K (2001) A sharp-interface-based approach to salt water intrusion problems: model development and applications. In: First International Conference on Saltwater Intrusion and Coastal Aquifers: Monitoring, Modeling, and Management, Essaouira, Morocco, April 2001

Cai X, McKinney DC, Lasdon LS (2001) Solving non-linear water management models using a combined genetic algorithm and linear programming approach. Adv Water Resour 24:667–676

Cheng AH-D, Halhal D, Naji A, Ouazar D (2000) Pumping optimization in saltwater-intruded coastal aquifers. Water Resour Res 36(8):2155–2165

Clerc M, Kennedy J (2002) The particle swarm: explosion, stability, and convergence in a multidimensional complex space. IEEE Trans Evol Comput 6(1):58–73

Dagan G, Zeitoun DG (1998) Seawater–freshwater interface in a stratified aquifer of random permeability distribution. J Contam Hydrol 29(3):185–203

del Valle Y, Venayagamoorthy GK, Mohagheghi S, Hernandez J-C, Harley RG (2008) Particle swarm optimization: basic concepts, variants and applications in power systems. IEEE Trans Evol Comput 12(2):171–195

Dhar A, Datta B (2009) Saltwater intrusion management of coastal aquifers, I: linked simulation-optimization. J Hydrol Eng 14(12):1263–1272

Diersch HJG, Kolditz O (2002) Variable-density flow and transport in porous media: approaches and challenges. Adv Water Resour 25(8–12):899–944

Dokou Z, Karatzas GP (2012) Saltwater intrusion estimation in a karstified coastal system using density-dependent modelling and comparison with the sharp-interface approach. Hydrol Sci J 57(5):985–999

Dokou Z, Karatzas GP (2013) Multi-objective optimization for free-phase LNAPL recovery using evolutionary computation algorithms. Hydrol Sci J 58(3):671–685

Dokou Z, Pinder GF (2011) Extension and field application of an integrated DNAPL source identification algorithm that utilizes stochastic modeling and a Kalman filter. J Hydrol 398(3–4):277–291

Eberhart R, Kennedy J (1995) A new optimizer using particle swarm theory. Proceedings of the 6th International Symposium on Micro Machine and Human Science, Nagoya, Japan, October 1995, pp 39–43

Elbeltagia E, Hegazy T, Grierson D (2005) Comparison among five evolutionary-based optimization algorithms. Adv Eng Inform 19:43–53

Finney BA, Samsuhadi Wills R (1992) Quasi-three-dimensional optimization model of Jakarta Basin. J Water Res Plan Manag 118(1):18–31

Gaur S, Chahar BR, Graillot D (2011) Analytic elements method and particle swarm optimization based simulation-optimization model for groundwater management. J Hydrol 402(3–4):217–227

Giambastiani BMS, Antonellini M, Essink GHPO, Stuurman RJ (2007) Saltwater intrusion in the unconfined coastal aquifer of Ravenna (Italy): a numerical model. J Hydrol 340(1–2):91–104

Gordon E, Shamir U, Bensabat J (2000) Optimal management of a regional aquifer under salinization conditions. Water Resour Res 36(11):3193–3203

Gorelick SM, Voss CI, Gill PE, Murray W, Saunders MA, Wright MH (1984) Aquifer reclamation design: the use of contaminant transport simulation combined with non-linear programming. Water Resour Res 20(4):415–427

Guvanasen V, Wade SC, Barcelo MD (2000) Simulation of regional ground water flow and salt water intrusion in Hernando County, Florida. Ground Water 38(5):772–783

Kallergis G, Lambrakis N, Voudouris K, Kokkalas S (2000) Hydrogeological investigation of the municipality of Malia area. University of Patras, Patras, Greece

Karterakis SM, Karatzas GP, Nikolos IK, Papadopoulou MP (2007) Application of linear programming and differential evolutionary optimization methodologies for the solution of coastal subsurface water management problems subject to environmental criteria. J Hydrol 342(3–4):270–282

Kopsiaftis G, Mantoglou A, Giannoulopoulos P (2009) Variable density coastal aquifer models with application to an aquifer on Thira Island. Desalination 237(1–3):65–80

Koukadaki MA, Karatzas GP, Papadopoulou MP, Vafidis A (2007) Identification of the saline zone in a coastal aquifer using electrical tomography data and simulation. Water Resour Manag 21(11):1881–1898

Kourakos G, Mantoglou A (2009) Pumping optimization of coastal aquifers based on evolutionary algorithms and surrogate modular neural network models. Adv Water Resour 32(4):507–521

Kourakos G, Mantoglou A (2011) Simulation and Multi-Objective Management of Coastal Aquifers in Semi-Arid Regions. Water Resour Manage 25:1063–1074

Llopis-Albert C, Pulido-Velazquez D (2014) Discussion about the validity of sharp-interface models to deal with seawater intrusion in coastal aquifers. Hydrol Process 28(10):3642–3654

Mantoglou A (2003) Pumping management of coastal aquifers using analytical models of saltwater intrusion. Water Resour Res 39(12)

Mantoglou A, Papantoniou M (2008) Optimal design of pumping networks in coastal aquifers using sharp interface models. J Hydrol 361:52–63

Mantoglou A, Papantoniou M, Giannoulopoulos P (2004) Management of coastal aquifers based on nonlinear optimization and evolutionary algorithms. J Hydrol 297(1–4):209–228

Matott LS, Rabideau AJ, Craig JR (2006) Pump-and-treat optimization using analytic element method flow models. Adv Water Resour 29(5):760–775

Milnes E, Renard P (2004) The problem of salt recycling and seawater intrusion in coastal irrigated plains: an example from the Kiti aquifer (southern Cyprus). J Hydrol 288(3–4):327–343

Papadopoulou MP, Nikolos IK, Karatzas GP (2010a) Computational benefits using artificial intelligent methodologies for the solution of an environmental design problem: saltwater intrusion. Water Sci Technol 62(7):1479–1490

Papadopoulou MP, Varouchakis EA, Karatzas GP (2010b) Terrain discontinuity effects in the regional flow of a complex karstified aquifer. Environ Model Assess 15(5):319–328

Pinder GF, Cooper HH (1970) A numerical technique for calculating transient position of saltwater front. Water Resour Res 6(3):875–882

Reilly TE, Goodman AS (1985) Quantitative-analysis of saltwater–freshwater relationships in groundwater systems: a historical perspective. J Hydrol 80(1–2):125–160

Reilly TE, Goodman AS (1987) Analysis of saltwater upconing beneath a pumping well. J Hydrol 89(3–4):169–204

Reinelt P (2005) Seawater intrusion policy analysis with a numerical spatially heterogeneous dynamic optimization model. Water Resour Res 41(5):1–12 W05006

Shamir U, Bear J, Gamliel A (1984) Optimal annual operation of a coastal aquifer. Water Resour Res 20:435–444

Tian N, Sun J, Xu WB, Lai CH (2011) An improved quantum-behaved particle swarm optimization with perturbation operator and its application in estimating groundwater contaminant source. Inverse Probl Sci Eng 19(2):181–202

Uddameri V, Kuchanur ZM (2007) Simulation-optimization approach to assess groundwater availability in Refugio County, TX. Environ Geol 51:921–929

Werner AD, Bakker M, Post VEA, Vandenbohede A, Lu C, Ataie-Ashtiani B, Simmons CT, Barry A (2013) Seawater intrusion processes, investigation, and management: recent advances and future challenges. Adv Water Resour 51:3–26

Willis R, Finney BA (1988) Planning model for optimal control of saltwater intrusion. J Water Res Plan Manag 114(2):163–178